Supplementary Information

SI–1 Measures of population structure in the island model

Here, I briefly discuss different measures of population structure in the infinite island model. In the Taylor-approximation for host fitness, we introduced $\mathrm{var}(q)$ as a measure of population structure. This is inline with the fact that for a given overall frequency of an allele (or strain) p, the classical measure of population structure, F_{st}, is given by [1] :

$$F_{st} = \frac{\mathrm{var}(q)}{p(1-p)} \,. \tag{SI–1}$$

In the island model, the probability that two individuals (sampled with replacement) in a given deme of local frequency q are of the same strain is given by $q^2 + (1-q)^2$. Taking the expectation of this over the Beta distribution (equation (SI–9)), we have the expected probability for two individuals from the same deme to be of the same strain as:

$$P(\text{same strain}) = \frac{1 + 2mn(1 - 2(1-p)p)}{1 + 2mn} \tag{SI–2}$$

Now, we assume that the probability that the second drawn individual is of the same type as the first one is given by a constant regression coefficient R plus $(1-R)$ times the frequency of the first drawn type in the population [2], we have:

$$P(\text{same strain}) = p(R + (1-R)p) + (1-p)(R + (1-R)(1-p)) \,, \tag{SI–3}$$

In general, this assumption is not guaranteed to hold, but in the infinite island model we can easily show that it does. Setting the right-hand sides of equations (SI–2) and (SI–3) equal to each other, and solving for R, we can show that R is indeed a frequency independent constant and equal to F_{st}:

$$R = \frac{1}{1 + 2mn} = F_{st}. \tag{SI–4}$$

The same relatedness coefficient can also be obtained as the low-migration, large deme limit of the probability that two randomly picked alleles will coalesce before leaving the deme when going backwards in time [3], which in the infinite island model with finite mutation is the identity by descent probability between two alleles (since coalescence can only occur within a deme). Our result is exact rather than an approximation, since we

only consider two alleles and ignore mutation.

SI–2 Full life-cycle in the island model

Here, I derive the expression for the change in frequency of the beneficial symbiont in an island model with weak selection. Consider a deme that contains the beneficial symbiont at frequency q. The fitness of the beneficial symbiont is given by:

$$\mathcal{W}_A = 1 + \delta w_A(q, s), \tag{SI–5}$$

and for the non-beneficial symbiont:

$$\mathcal{W}_B = 1 + \delta w_B(q, s)\,, \tag{SI–6}$$

where $\delta \ll 1$ is the strength of selection. The new local frequency of the beneficial symbiont, after selection and migration is:

$$q' = (1-m)\frac{q\mathcal{W}_A}{q\mathcal{W}_A + (1-q)\mathcal{W}_B} + m\frac{\int_0^1 q\mathcal{W}_A f(q|p)dq}{\int_0^1 \big(q\mathcal{W}_A + (1-q)\mathcal{W}_B\big) f(q|p)dq}\,, \tag{SI–7}$$

where m the the probability of new individuals in a patch being migrants. Taking the Taylor expansion to first order in δ, and integrating over $f(q|p)$, we find the new overall frequency of the beneficial symbiont, p':

$$p' \approx p + \delta \int_0^1 \Big[\big((1-m)q(1-q) + mq(1-p)\big)w_A(q,s) - \big((1-m)q(1-q) + mp(1-q)\big)w_B(q,s)\Big] f(q|p)dq\,. \tag{SI–8}$$

Finally, I assume selection is weak enough that the distribution of the local deme frequencies of the beneficial symbiont, $f(q|p)$, is well-approximated by neutrality [4]. Thus, we have:

$$f(q|p) = \frac{1}{B(\alpha,\beta)} q^{\alpha-1}(1-q)^{\beta-1}\,, \tag{SI–9}$$

where $B(\cdot,\cdot)$ is the Beta function, $\alpha = nmp$, $\beta = nm(1-p)$, and n is the symbiont deme size.

Local competition changes the results reported in the main text section 4.1 and 4.2 in

substantive ways. Under fixed rewards, population structure has no influence on whether selection favors the cooperative symbiont or not: there exist a threshold level of choosiness independent of population structure above which the beneficial symbiont is favored, and below which it is not (Supplementary Figure 1, left-hand panel). This is a case of fertility effects of population structure being cancelled out exactly by the local competition effect [5]. On the other hand, under feedback-dependent rewards, population structure helps the beneficial symbiont at high levels of choosiness while hurting it at low levels (Supplementary Figure 1, right-hand panel). In particular, there exists a (low to moderate) range of host choosiness where the beneficial symbiont goes from being favored only when common to never being favored as population structure increases, whereas at higher host choosiness levels the symbiont goes to being always favored. Interestingly, and in contrast to the results without local competition, this pattern holds regardless of the shape of the host benefit. The reason local competition does not exactly cancel out the fertility effects under feedback-dependent but not fixed rewards is that in the former, there are effectively two social interactions involved: the first is partner choice, while the second is a public goods game through the host. Due to partner choice, the second stage happens over a modified distribution of strain frequencies relative to the distribution over which the local competition happens, therefore the the latter does not entirely cancel the former: when choosiness is low, local competition becomes more important as population structure increases, whereas when choosiness is high enough, the benefits from the public goods rewards become more important.

SI–3 Coevolutionary model

1 Host fitness in the coevolutionary model

In this section, I describe the model where two genotypes each of the host and symbiont exist in the population. One of the host genotypes has choosiness s and the other zero (i.e., does not reject any symbiont). I assume that the choosy host's fitness when the local frequency of the beneficial symbiont is q is given by

$$\mathcal{W}_{ch} = 1 + \delta w_h(q, s) \,, \tag{SI–10}$$

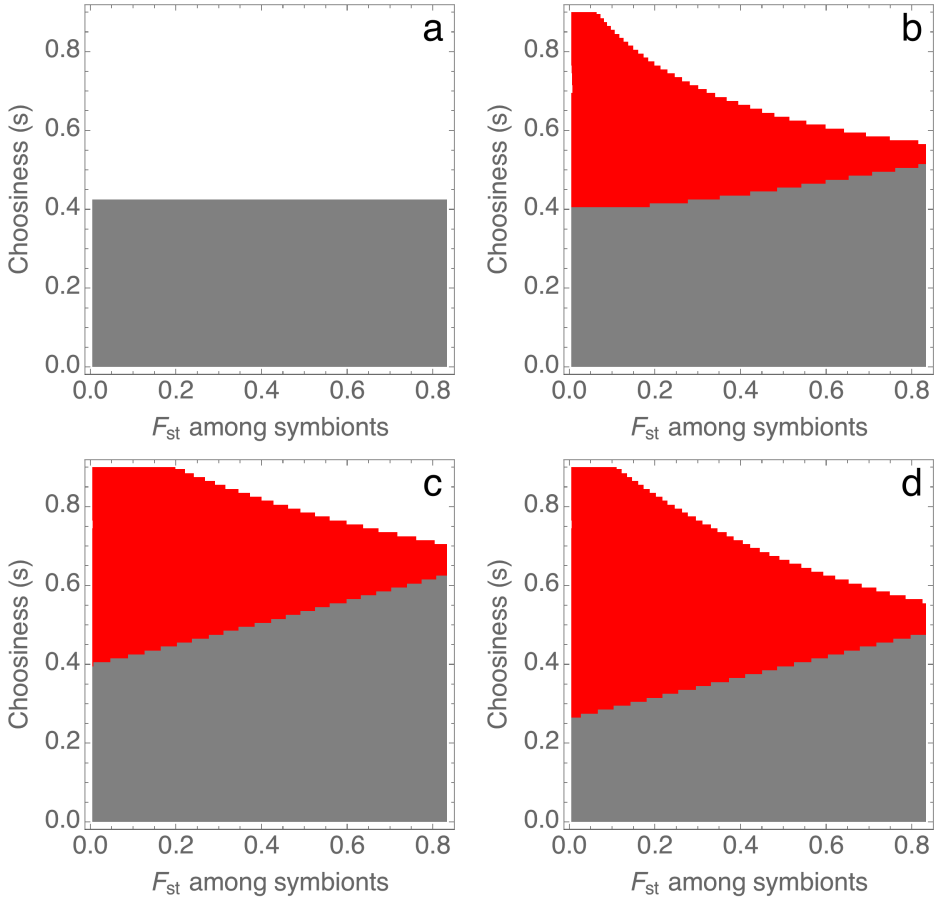

Supplementary Figure 1: Effect of population structure changes when local competition is taken into account. Colors as in Figures 3 and 4 in the main text (gray=beneficial symbiont does not invade or fix, white=beneficial symbionts invades and fixes, red=beneficial symbiont cannot invade but can fix). Panel a depicts the fixed rewards ($h_0 = 1$, $h_1 = 0$) case: population structure has no effect on selection in the symbiont population. Other panels depict the feedback-dependent reward cases ($h_0 = 0$, $h_1 = 1$) with different shapes of host benefit. The all show that with high host choosiness, population structure helps the beneficial symbiont getting selected for at low frequencies while for lower host choosiness, the symbiont goes from being favored when common to not being favored ay any frequency. Particular host benefit functions are as follows. Panel b: diminishing returns ($b(q_c) = q_c - q_c^2/2$), c: linear returns ($b(q_c) = q_c$), d: accelerating returns ($b(q_c) = q_c + q_c^2/2$). In all panels $k = 0.4$ and $n = 100$, except for the diminishing rewards (panel b), where $k = 0.2$.

where δ is the strength of selection, assumed to be small, w_h is given by equation (2), and I assume a linear cost to choosiness:

$$c(s) = \chi s \,, \tag{SI–11}$$

with χ a constant. The fitness of a non-choosy host is:

$$\mathcal{W}_{nh} = 1 + \delta w_h(q, 0) \,. \tag{SI–12}$$

As in section SI–2, I assume the hosts also live in an island structured population, with n_h the host deme size, and m_h the fraction of each deme that is formed from the global migrant pool. The analysis will then proceed as above Because of the weak selection assumption, I use the neutral distribution of local frequencies for both the host and symbiont [e.g. 4, 6]. The weak selection assumption also allows me to neglect potential build up of correlations between host and symbiont genotypes [7] so that the joint local frequency distributions of hosts and symbionts are given just by the product of their separate distributions. The overall frequency of choosy hosts in the global migrant pool after selection is:

$$\frac{\int_0^1 q_h \mathcal{W}_{ch} f(q|p) g(q_h|p_h) dq dq_h}{\int_0^1 \big(q_h \mathcal{W}_{ch} + (1 - q_h)\mathcal{W}_{nh}\big) f(q|p) g(q_h|p_h) dq dq_h} \,, \tag{SI–13}$$

which to first order in the strength of selection becomes:

$$p_h + \delta p_h (1 - p_h) \int_0^1 (w_h(q, s) - w_h(q, 0)) f(q|p) dq \,. \tag{SI–14}$$

Meanwhile, the contribution of the philopatric individuals to first order in δ is:

$$\int_0^1 \int_0^1 (q_h + \delta q_h (1 - q_h)(w_h(q, s) - w_h(q, 0)) f(q|p) g(q_h|p_h) dq dq_h \,. \tag{SI–15}$$

Observe that $w_h(q, s) - w_h(q, 0)$ is not a function of q_h, so the only dependence to q_h is in the q_h and $q_h(1 - q_h)$ terms. Thus, we can take the q_h integral easily to obtain:

$$(p_h - \mathrm{var}(q_h) - p_h^2) \int_0^1 (w_h(q, s) - w_h(q, 0)) f(q|p) dq \,. \tag{SI–16}$$

The total frequency of the choosy hosts in the next generation is expression (SI–14) times m_h plus expression (SI–16) times $(1 - m_h)$, hence:

$$p'_h \approx p_h + \delta(m_h p_h(1-p_h) + (1-m_h)(p_h + \mathrm{var}(q_h) - p_h^2)) \int_0^1 (w_h(q,s) - w_h(q,0)) f(q|p) dq \,. \tag{SI–17}$$

Note that, unlike equation (4), this expression is *not* a low-variance approximation in either q or q_h (we only assumed small δ, i.e. weak selection). The term $\mathrm{var}(q_h)$ arises because the q_h dependency of the integrand is quadratic, so can be expressed exactly using the second moment of $g(q_h|p_h)$. To calculate $\mathrm{var}(q_h)$, I assume that the local choosy host frequency distribution is given by:

$$g(q_h|p_h) = \frac{1}{B(\alpha_h, \beta_h)} q_h^{\alpha_h - 1} (1-q_h)^{\beta_h - 1} \,, \tag{SI–18}$$

where $\alpha_h = n_h p_h$, $\beta_h = n_h(1-p_h)$, n_h are the symbiont and host deme sizes, respectively [4]. The symbiont local frequency distribution $f(q|p)$ is again given by (SI–9).

2 Symbiont fitness in the coevolutionary model

Now I turn to the symbiont fitness. In a deme that contains the beneficial symbiont at frequency q and the choosy host at q_h, the fitness of the beneficial symbiont is given by:

$$\mathcal{W}_A = 1 + \delta(q_h w_A(q,s) + (1-q_h) w_A(q,0)) \,, \tag{SI–19}$$

and for the non-beneficial symbiont:

$$\mathcal{W}_B = 1 + \delta(q_h w_B(q,s) + (1-q_h) w_B(q,0)) \,. \tag{SI–20}$$

The new local frequency of the beneficial symbiont, after selection and migration is:

$$q' = (1-m)\frac{q\mathcal{W}_A}{q\mathcal{W}_A + (1-q)\mathcal{W}_B} + m\frac{\int_0^1 \int_0^1 q\mathcal{W}_A f(a) g(q_h|p_h) dq dq_h}{\int_0^1 \int_0^1 \big(q\mathcal{W}_A + (1-q)\mathcal{W}_B\big) f(a) g(q_h|p_h) dq dq_h} \tag{SI–21}$$

Taking the Taylor expansion to first order in δ, and integrating over $f(q|p)$ and $g(q_h|p_h)$, we find the new overall frequency of the beneficial symbiont, p':

$$p' \approx p + \delta \int_0^1 \int_0^1 \Big[\big((1-m)q(1-q) + mq(1-p)\big) u_A(q, q_h) - \big((1-m)q(1-q) + mp(1-q)\big) u_B(q, q_h) \Big] f(q|p) g(q_h|p_h) dq dq_h \,, \quad \text{(SI–22)}$$

where $u_A(q, q_h) = q_h w_A(q, s) + (1-q_h) w_A(q, 0)$ and $u_b(q, q_h) = q_h w_B(q, s) + (1-q_h) w_B(q, 0)$, i.e., the expected fitness increments to each strain due to the interactions in the local deme. This means that the integrand in (SI–22) is linear in q_h, so the q_h integral can again be taken easily to obtain:

$$p' \approx p + \delta \int_0^1 \int_0^1 \Big[\big((1-m)q(1-q) + mq(1-p)\big) u_A(q, p_h) - \big((1-m)q(1-q) + mp(1-q)\big) u_B(q, p_h) \Big] f(q|p) dq \,, \quad \text{(SI–23)}$$

in other words, we can simply evaluate the fitness increments for each strain at the global mean frequency of the choosy hosts.

Below, I sketch out the general patterns of the coevolutionary dynamics of the choosy host and beneficial symbiont frequencies, starting with fixed rewards to the symbiont.

3 Fixed rewards to the symbiont

The first finding for fixed rewards to the symbionts is that there exists parameter combinations for which polymorphisms in both host and the symbiont are stably maintained, even in the absence of mutational (or migrational) input which most previous research has suggested to be important. However, the equilibrium where the beneficial symbiont and choosy hosts go extinct also is always stable. Stronger population structure of symbionts shrinks the basin of attraction of the stable equilibrium and shifts the equilibrium frequencies of the beneficial symbiont and choosy hosts lower, as shown in Figure 5 in the main text, which depicts the case where host fitness is a linear function of q_c, and Figure 6, also in the main text, which depicts how the equilibrium frequency changes with population structure.

This pattern stays largely the same when host benefit exhibits diminishing or accelerating returns to q_c (Supplementary Figure **??**), although with diminishing returns, population structure can initially increase the equilibrium frequency of the beneficial symbiont

(Supplementary Figure 3). Accelerating returns tend to make the cycles larger for the same parameter set.

To summarize, the overall effect of population structure in the fixed rewards case is to reduce the amount and likelihood of stable cooperation. The model also predicts that the coexistence patterns will generally exhibit at least transitory cycling when starting in the interior, either as oscillatory convergence to the stable equilibrium or as limit cycles. This is in line with previous results [8, 9].

4 Feedback-dependent rewards

The pattern with feedback-dependent rewards is broadly similar to fixed rewards. The boundary equilibrium without the beneficial symbiont and choosy host is again always stable. There can also be an internal equilibrium as in the fixed-rewards case, but for the same host benefit functions a higher level of host choosiness is required for this equilibrium to be stable. Population structure has the same effects as in the fixed-rewards case: it shrinks the basin of attraction of the stable equilibrium, eventually removing the stable equilibrium (Supplementary Figure 4), while also generally tending to reduce the frequency of cooperation and choosiness (Supplementary Figure 5).

SI–4 Strong selection simulations

In this section, I describe the results of stochastic simulations of the island model under strong selection. The basic life-cycle is as in the analytical model above, except there are a finite (large) number of demes. Strong selection allows the build-up of covariances between the frequencies of different host and symbiont genotypes across demes and therefore host population structure will not be neutral anymore.

References cited in the Supplementary Information

[1] Wright S. Evolution in Mendelian populations. *Genetics* **16** (1931), 97.

[2] Rousset F, Billiard S. A theoretical basis for measures of kin selection in subdivided populations: Finite populations and localized dispersal. *J. Evol. Biol.* **13** (2000), 814–825.

[3] Rousset F. *Genetic Structure and Selection in Subdivided Populations*. Ed. by Levin SA, Horn HS. Princeton: Princeton University Press, 2004.

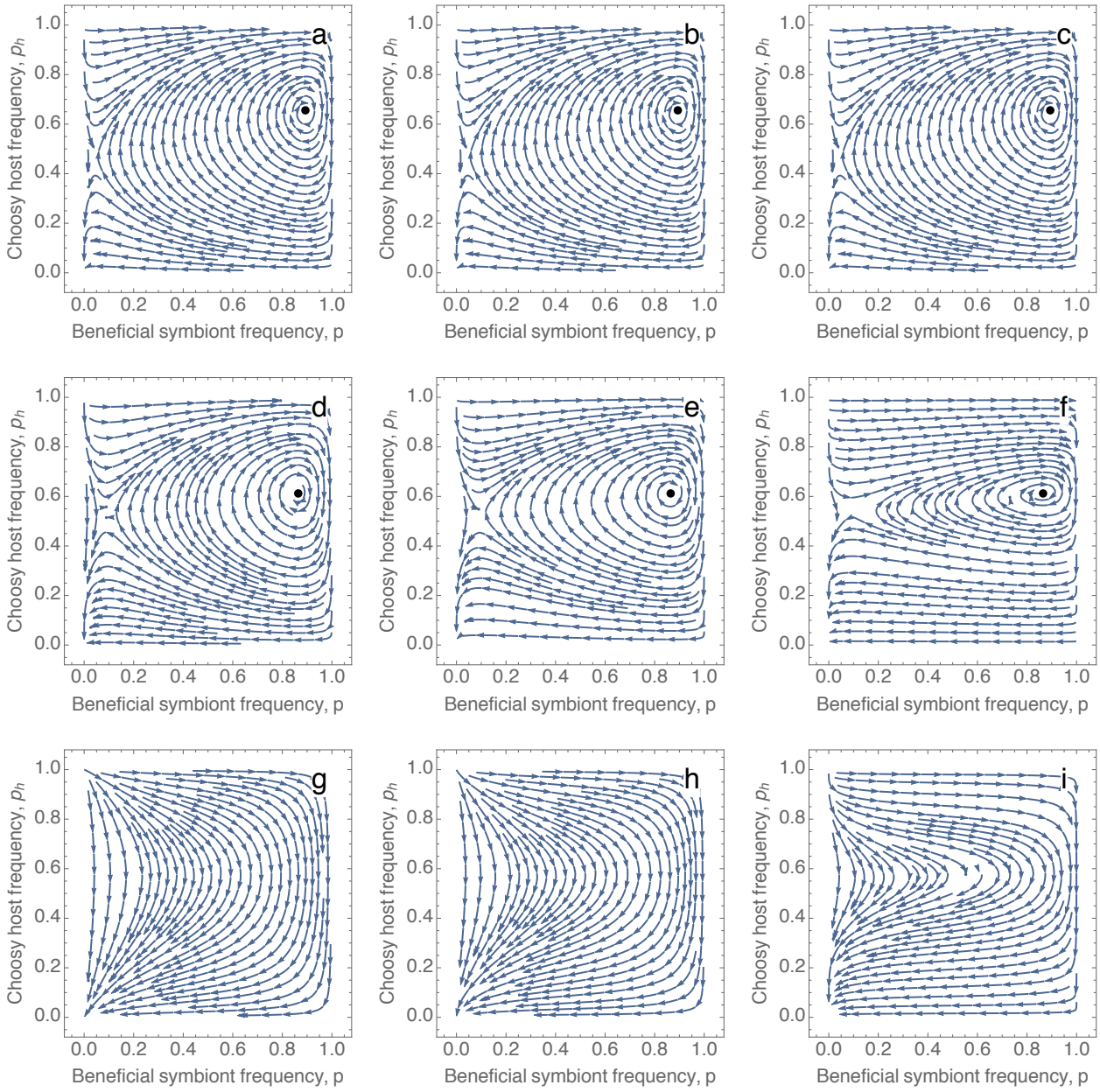

Supplementary Figure 2: Population structure in both hosts and symbionts disfavors choosiness and cooperation with fixed rewards. The panels depict variation in the co-evolutionary dynamics of cooperation and choosiness as a function of the migration rates m and m_h of the symbionts and hosts, respectively. Rows correspond to (from top to bottom) $m = 1$, $m = 0.01$, and $m = 0.001$, respectively; columns (from left to right) $m_h = 1$, $m_h = 0.01$, $m_h = 0.001$, respectively. In all panels, the boundary equilibrium at $(0, 0)$ is locally stable. Host population structure has no effect when symbiont population is well mixed (top row), but reduces the basin of attraction of the stable equilibrium when symbiont population is structured (middle row). Symbiont population structure for all host migration rates causes the stable internal equilibrium to support less cooperation, reduces the basin of attraction of this equilibrium, and eventually makes it disappear. Other parameters are: $h_0 = 1$, $h_1 = 1$, $b(q_c) = q_c$, $s = 0.6$, $\chi = 0.1$, $n = n_h = 100$.

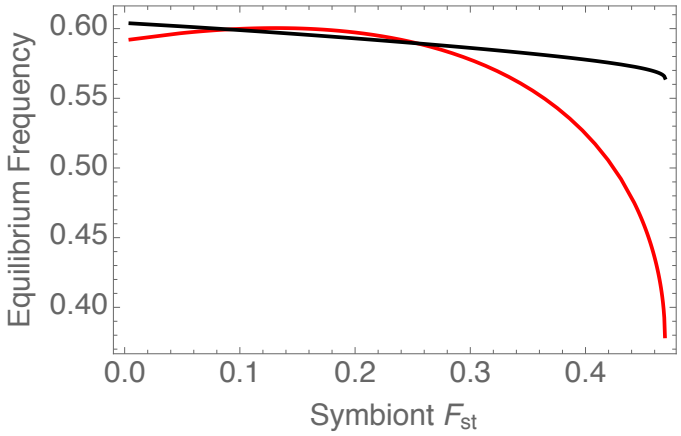

Supplementary Figure 3: With diminishing returns to the host and fixed rewards to the symbiont, population structure might first increase, then decrease the frequency of the beneficial symbiont. Red curve gives the equilibrium frequency of the beneficial symbiont; black the choosy host. Parameters as in Supplementary Figure **??**.

[4] Cherry JL, Wakeley J. A diffusion approximation for selection and drift in a subdivided population. *Genetics* **163** (2003), 421–428.

[5] Taylor PD. Inclusive fitness in a homogeneous environment. *Proceedings of the Royal Society of London B: Biological Sciences* **249** (1992), 299–302.

[6] Wright S. The genetical structure of populations. *Annals of eugenics* **15** (1951), 323–354.

[7] Frank S. Genetics of mutualism: the evolution of altruism between species. *Journal of Theoretical Biology* **170** (1994), 393–400.

[8] Steidinger BS, Bever JD. The coexistence of hosts with different abilities to discriminate against cheater partners: an evolutionary game-theory approach. *The American Naturalist* **183** (2014), 762–770.

[9] Ezoe H. Coevolutionary dynamics in one-to-many mutualistic systems. *Theoretical Ecology* (2016), 1–8.

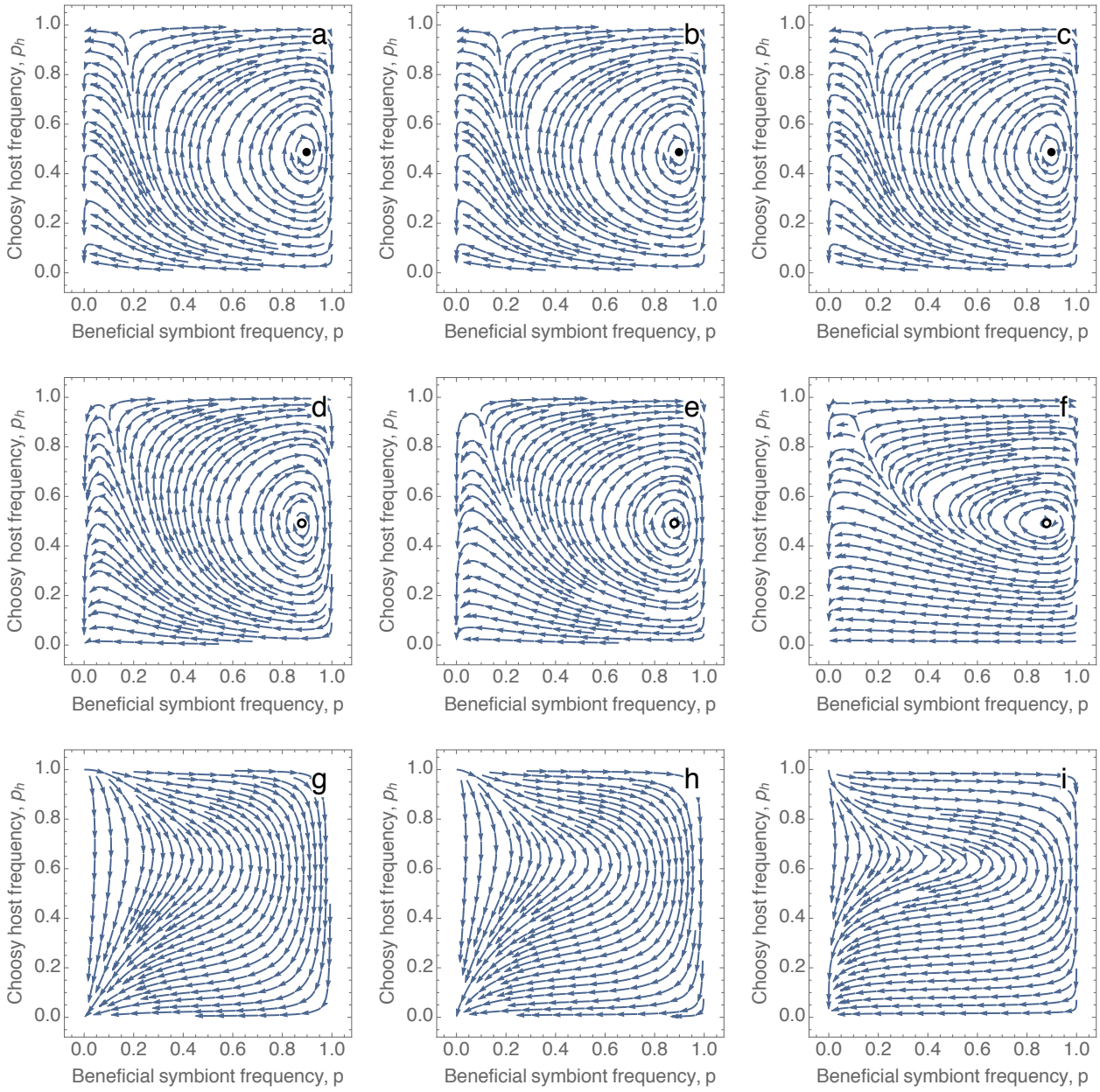

Supplementary Figure 4: Population structure in both hosts and symbionts disfavors choosiness and cooperation with fixed rewards. As in Figure 2, the rows and columns are for decreasing m and m_h values, respectively (1, 0.01, and 0.001). Filled black circles depict stable internal equilibria, file open circles depict unstable internal equilibria. In all panels, the boundary equilibrium at $(0, 0)$ is locally stable. Increasing symbiont population structure (decreasing m) causes this equilibrium to be first unstable (middle row, see also Figure 5) and then disappear (bottom row). This figure assumes linear benefits to the host ($b(q_c) = q_c$) and feedback-dependent symbiont rewards ($h_0 = 0$, $h_1 = 1$). Host choosiness is $s = 0.8$; $m = 1$ on the left-hand panel; $m = 0.001$ on the right-hand. Other parameters: $\chi = 0.1$, $k = 0.4$, $n = n_h = 100$, $m_h = 1$.

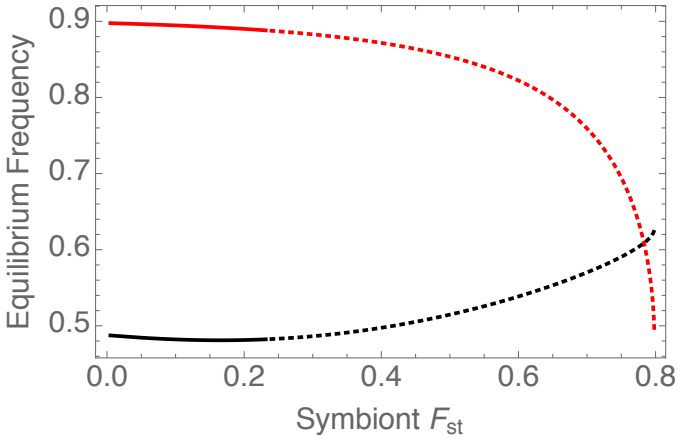

Supplementary Figure 5: Symbiont population structure decreases the equilibrium frequency of the beneficial symbiont and increases the frequency of the choosy host with feedback dependent rewards. Population structure can also destabilizes the internal equilibrium (as determined by the dominant eigenvector of the Jacobian matrix being greater than 1); the unstable equilibrium is indicated by the dotted curves above a threshold F_{st} value. For this figure, we assumed linear benefits to the host ($b(q_c) = q_c$) and feedback-dependent symbiont rewards ($h_0 = 0$, $h_1 = 1$). Other parameters as in Supplementary Figure 4.

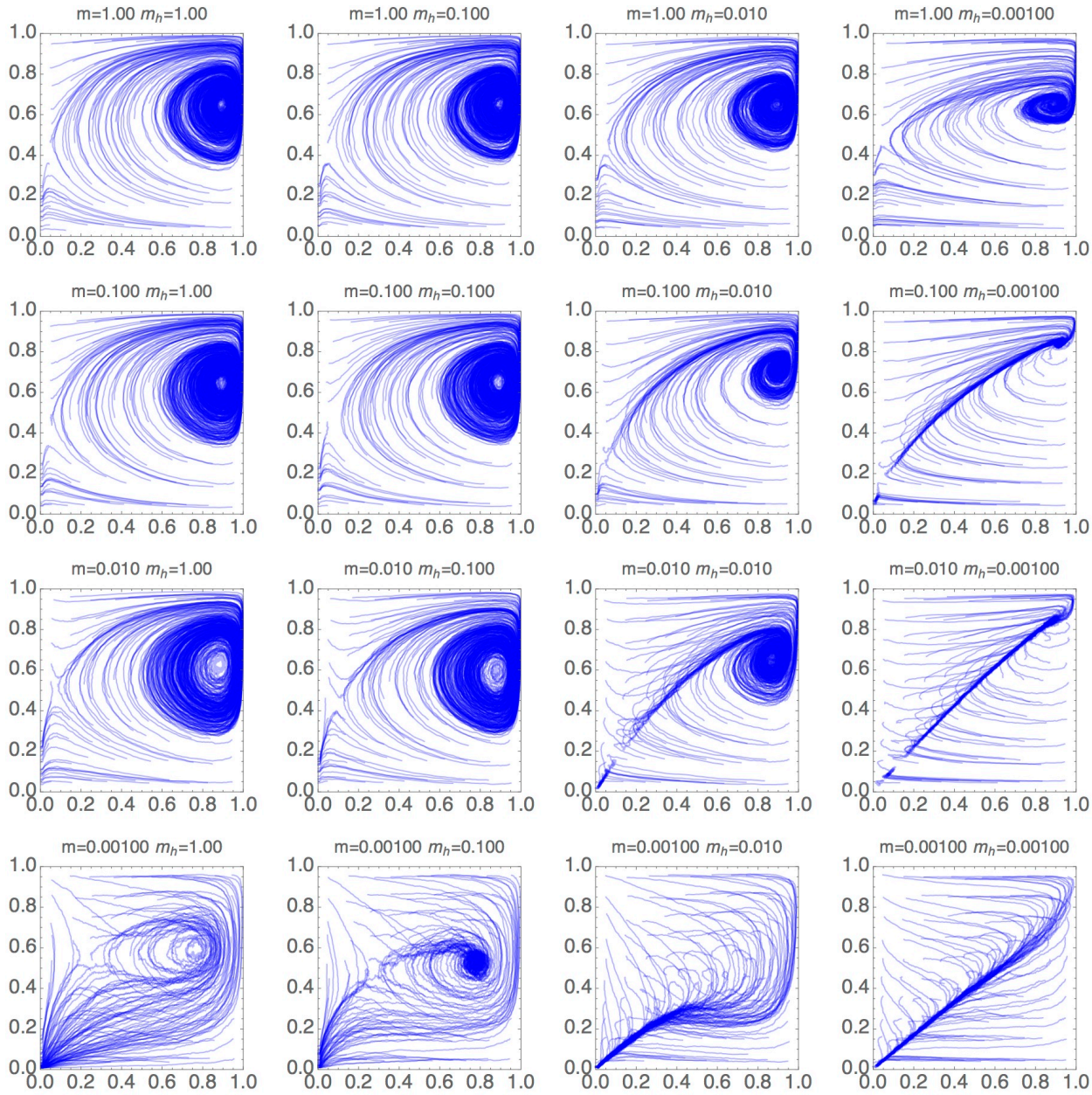

Supplementary Figure 6: Simulations of the island model with strong selection ($\delta = 0.5$) while varying the migration rates of the hosts and symbionts (given at the top of each panel). For each pair of migration rates m and m_h, I simulated 100 populations consisting of 1000 demes of 100 hosts and symbionts each, with starting frequencies p and p_h on a grid $[0.05, 0.95]$ for both. Each blue curve corresponds to the trajectory of one such population, for 1000 time steps. This graph is for fixed rewards $h_0 = 1$, $h_1 = 0$, and linear host fitness $b(q_c) = q_c$. Other parameters are $s = 0.6$, $\chi = 0.1$.

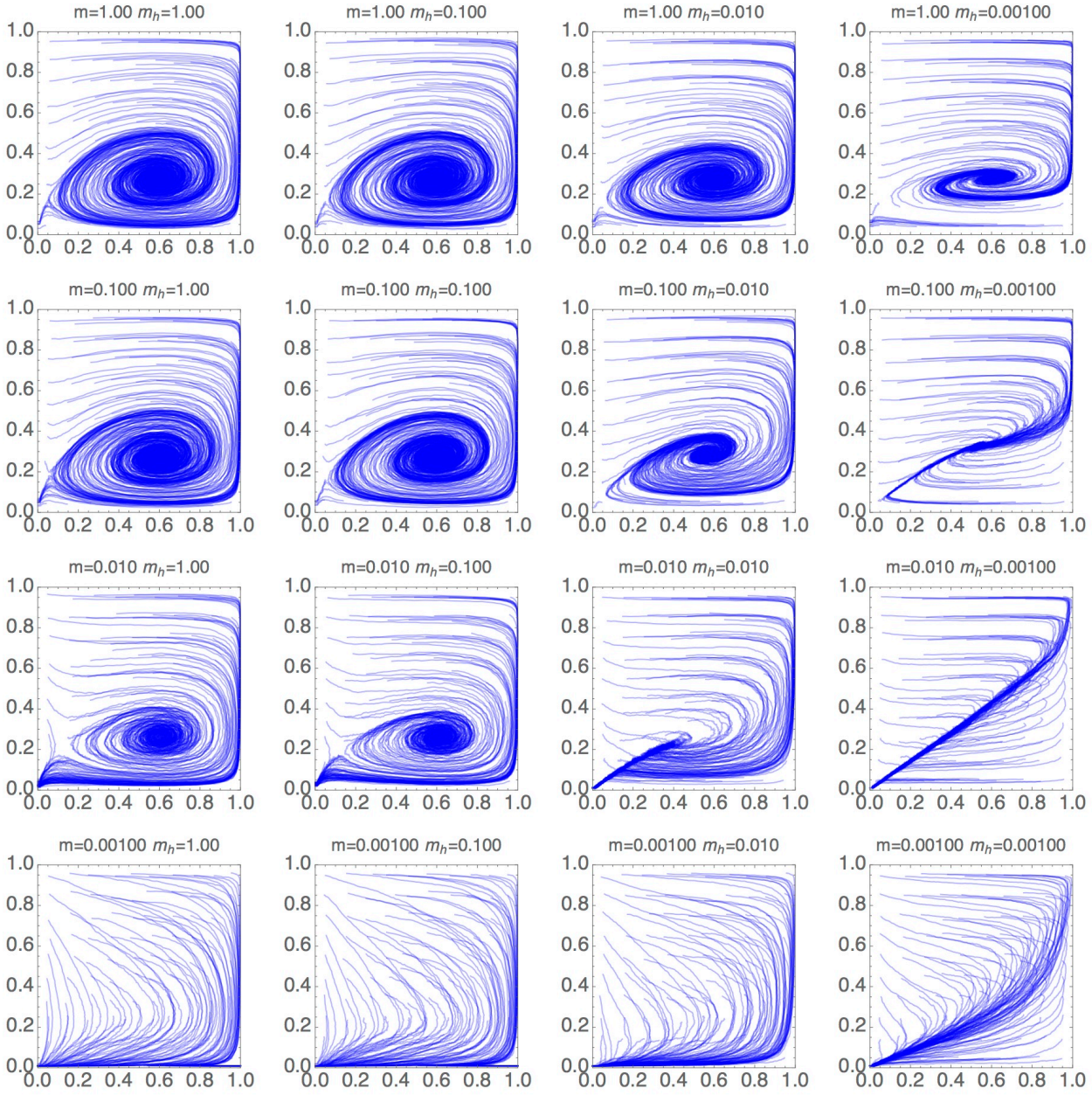

Supplementary Figure 7: Simulations of the island model with strong selection ($\delta = 0.5$) while varying the migration rates of the hosts and symbionts (given at the top of each panel). Simulation procedure as in Figure . This graph is for feedback-dependent rewards $h_0 = 0$, $h_1 = 1$, and diminishing returns host fitness $b(q_c) = q_c - q_c^2/2$. Other parameters are $s = 0.6$, $\chi = 0.1$. For weak symbiont population structure (top two rows), host population structure has no or positive effect on the maintenance of cooperation. However, in the third row, going right, one can see that strong host population structure can cause a stable equilibrium to disappear.

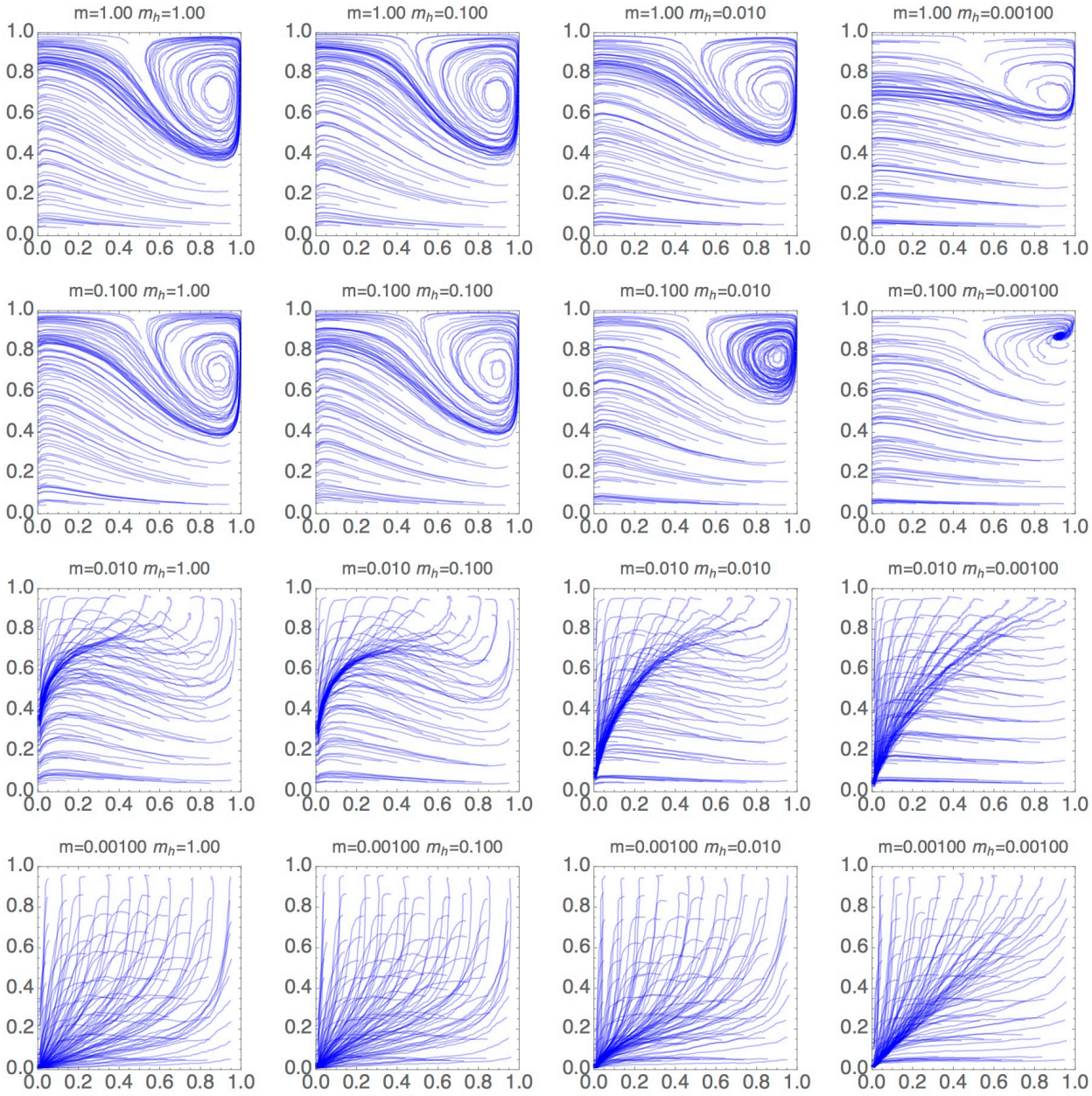

Supplementary Figure 8: Simulations of the island model with strong selection ($\delta = 0.5$) while varying the migration rates of the hosts and symbionts (given at the top of each panel). Simulation procedure as in Figure . This graph is for feedback-dependent rewards ($h_0 = 0$, $h_1 = 1$), and linear host fitness ($b(q_c) = q_c$). Other parameters are $s = 0.6$, $\chi = 0.1$. In the second row, going right, one can observe that strong host population structure can cause the internal equilibrium to become stable.

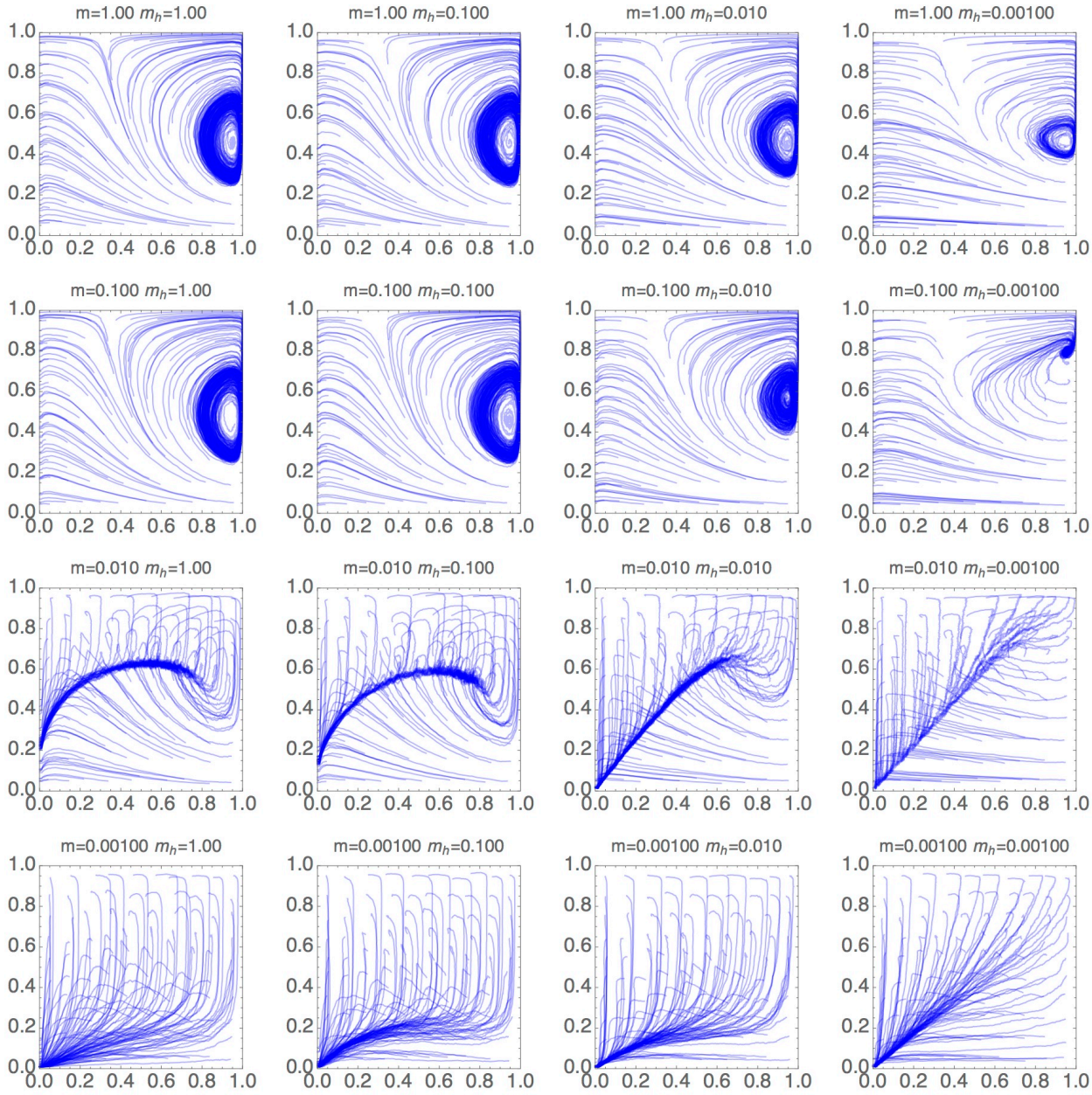

Supplementary Figure 9: Simulations of the island model with strong selection ($\delta = 0.5$) while varying the migration rates of the hosts and symbionts (given at the top of each panel). Simulation procedure as in Figure . This graph is for feedback-dependent rewards ($h_0 = 0$, $h_1 = 1$), and accelerating host fitness ($b(q_c) = q_c + q_c^2/2$). Other parameters are $s = 0.6$, $\chi = 0.1$. With weak symbiont population structure (top two rows), stronger host population structure tends to shrink the basin of attraction of the stable equilibrium.